Acta Crystallographica Section B
Structural Science
ISSN 0108-7681

Solid-state structures of the covalent hydrides germane and stannane

Iain J. Maley,[a] Daniel H. Brown,[a] Richard M. Ibberson[b]* and Colin R. Pulham[a]

[a]School of Chemistry, The University of Edinburgh, King's Buildings, West Mains Road, Edinburgh EH9 3JJ, Scotland, and [b]ISIS Facility, STFC, Rutherford Appleton Laboratory, Harwell Science and Innovation Campus, Didcot OX11 0QX, England

Correspondence e-mail: r.m.ibberson@rl.ac.uk

Received 30 October 2007
Accepted 15 April 2008

The low-temperature crystal structures of perdeuterogermane (m.p. 108 K) and perdeuterostannane (m.p. 123 K) are reported. The structures have been characterized from low-temperature (5 K) high-resolution neutron powder diffraction experiments following sample preparation using *in situ* gas-condensation techniques. GeD_4 crystallizes in an orthorhombic structure, space group $P2_12_12_1$, with one molecule in the asymmetric unit, and with an average Ge—D bond length of 1.517 (3) Å. The SnD_4 structure is monoclinic (space group $C2/c$), and the molecule is located on a twofold rotation axis with an average Sn—D bond length of 1.706 (3) Å. The crystal structures are discussed in relation to those of other tetrahedral molecules of group IV hydrides at low temperature, and evidence is presented that the crystal structure of silane, below 38 K, is isostructural with germane.

1. Introduction

The group IV hydrides have attracted attention recently following the suggestion by Ashcroft (2004) that the 'chemically pre-compressed' hydrogen in these alloys may promote metallization, making them candidate materials for high-T_c superconductors at pressures achievable in diamond–anvil cells. Initial theoretical studies on silane, SiH_4 (Feng *et al.*, 2006), have been followed by first-principles calculations on GeH_4 (Li *et al.*, 2007; Martinez-Canales *et al.*, 2006) and most recently on SnH_4 (Tse *et al.*, 2007). However, little is known about the solid-state structures of these compounds, under either ambient or high-pressure conditions.

In the case of silane, three phases have been reported following X-ray (Sears & Morrison, 1975) and neutron powder diffraction (Legrand & Press, 1976). The phase I structure is most likely tetragonal and is stable between the melting point at 89 K and down to 64 K. No structural information is available for phase II or phase III, the latter is thought to be stable below 38 K. A high-pressure monoclinic phase of silane has recently been observed and solved between 10 and 25 GPa (Degtyareva *et al.*, 2007). There are no reports of crystal structure information for solid germane or stannane; however, an extensive literature regarding spectroscopic studies and physical property measurements is available for these compounds and their perdeuterated isotopologues. In the case of germane, heat-capacity measurements (Clusius & Faber, 1942; Mountfield & Weir, 1978) detect the presence of three λ-type transitions at 63, 74 and 77 K between the melting point at 107 and 3 K. NMR measurements on polycrystalline GeD_4 (Hovi *et al.*, 1969) suggest that the transitions at 78 and 75 K are first-order and associated with ordering of molecular reorientation; however, the 68 K transition is of higher order. IR spectra of solid germane (McKean & Chalmers, 1967; The

Table 1
Experimental details.

Lattice parameters determined at the condensation temperatures are given in the deposited CIF file.

	Germane	Stannane
Crystal data		
Chemical formula	D_4Ge	D_4Sn
M_r	80.65	126.75
Cell setting, space group	Orthorhombic, $P2_12_12_1$	Monoclinic, $C2/c$
Temperature (K)	5	5
a, b, c (Å)	7.35565 (17), 8.15934 (11), 4.53932 (11)	8.87431 (14), 4.54743 (7), 8.75705 (12)
β (°)	90	119.2882 (10)
V (Å^3)	272.44 (1)	308.22 (1)
Z	4	4
D_x (Mg m^{-3})	1.966	2.731
Radiation type	Time-of-flight neutron	Time-of-flight neutron
Powder preparation temperature (K)	65	75
Data collection		
Diffractometer	HRPD	HRPD
Data collection method	Specimen mounting: standard cylindrical vanadium sample holder; scan method: TOF† range 30–130 ms	Specimen mounting: standard cylindrical vanadium sample holder; scan method: TOF† range 30–130 ms
$\langle 2\theta \rangle$ (°)	168	168
Refinement		
Refinement on	Rietveld method	Rietveld method
R factors and goodness of fit	R_p = 0.061, R_{wp} = 0.069, R_{exp} = 0.043, S = 1.60	R_p = 0.111, R_{wp} = 0.124, R_{exp} = 0.062, S = 2.03
Wavelength of incident radiation (Å)	1.2–5.2	1.2–5.2
Excluded region(s)	96–104 ms	96–104 ms
Profile function	TOPAS TOF pseudo-Voigt	TOPAS TOF pseudo-Voigt
No. of parameters	45	35
D-atom treatment	All D-atom parameters refined	All D-atom parameters refined
Weighting scheme	Based on measured s.u.'s	Based on measured s.u.'s
$(\Delta/\sigma)_{max}$	0.01	0.02
Preferred orientation correction	Spherical harmonic order = 6	Spherical harmonic order = 6

Computer programs used: *TOPAS-Academic* (Coehlo, 2008), standard HRPD normalization routines. † TOF = time of flight.

et al., 1974) were interpreted on the basis of four phases; however, subsequent studies (Oxton, 1977; Calvani *et al.*, 1990, 1991) questioned the existence of a fourth phase with symmetry lower than that of phase III. In the case of stannane, its lability represents a major difficulty for solid-state studies. NMR studies in the range 68–129 K reveal a phase transition at 98 K for SnH_4 (Niemela *et al.*, 1972) and at 103 K for the deuterated analogue (Niemela, 1973). No spectroscopic evidence for a transition point was found using IR spectroscopy (McKean & Chalmers, 1967). Isotope effects on the phase-transition sequences of silane, germane and stannane are seen to increase the transition points by up to 5 K for the perdeuterated isotopologues as outlined above. There is currently no evidence supporting isotopic polymorphism in these hydrides.

The dearth of information about the solid-state structures of these very simple compounds stems in part from the difficulties involved in obtaining suitable single crystals from compounds that are gases under ambient conditions, and which solidify only at very low temperatures. This position is now changing, however, with the development of techniques for *in situ* growth of crystals from liquids with low melting points (Boese & Nussbaumer, 1994). In a typical experiment, the liquid sample is contained within a sealed capillary mounted in a thermally insulating support, which is in turn mounted on the goniometer of an X-ray diffractometer. By judicious warming and cooling of the sample just below its melting point, a single crystal can be grown *in situ* with X-ray data being collected in the normal way. Thus, the solid-state structures of hydride derivatives such as $AlMe_2BH_4$ and $Al(BH_4)_3$ (Aldridge *et al.*, 1997), and H_2GaBH_4 (Downs *et al.*, 1997) have been determined successfully by single-crystal X-ray diffraction. A recurring theme in these structures is one of intermolecular interactions involving bridging H atoms resulting in the adoption of polymeric structures. In contrast, the structures of hydride derivatives of the heavier Group 14 elements have scarcely been investigated. A single-crystal X-ray diffraction study of GeH_3Cl (Blake *et al.*, 1987) showed the presence of strong Ge···Cl intermolecular interactions.

Attempts to grow single crystals of stannane at low temperatures from the liquid sealed in glass capillaries failed on account of the very low melting point of stannane (123 K), making it difficult to maintain the temperature gradients required for high-quality crystal growth. Since germane has an even lower melting point (108 K), no attempts at single-crystal growth were made. Prompted by the fundamental nature of these hydrides and the current level of interest, the crystal structures of the low-temperature phases of perdeuterogermane and -stannane have now been investigated using high-resolution neutron powder diffraction.

2. Experimental

2.1. Sample preparation

Samples of perdeuterated germane, GeD_4, and stannane, SnD_4, were prepared from the respective tetrahalides and lithium aluminium deuteride (Aldrich 98 D-atom %) according to standard procedures. Powder samples were produced using a vapour-deposition technique as follows. The samples were prepared in a standard vanadium-tailed liquid-helium 'orange' cryostat using a centre stick incorporating a

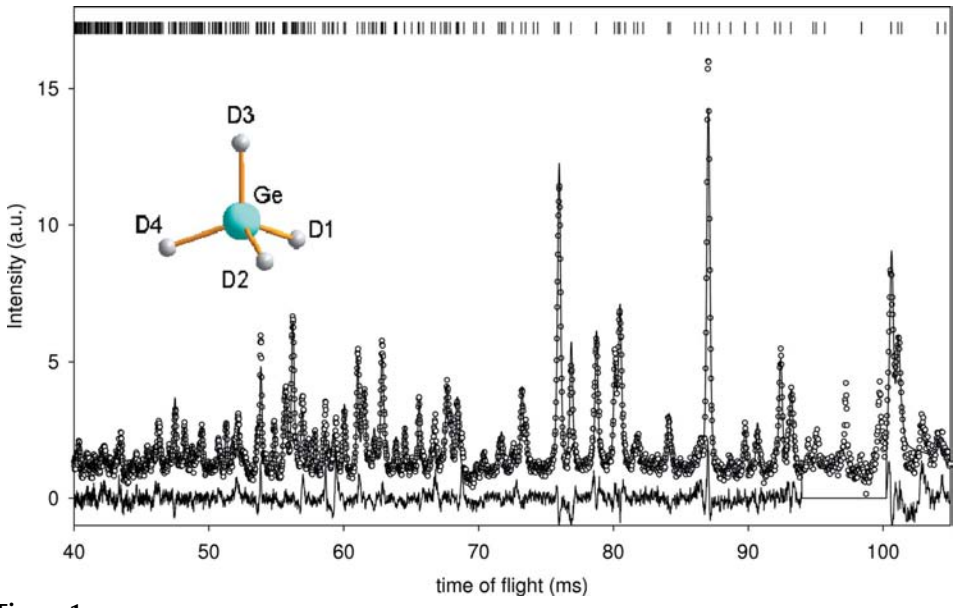

Figure 1
The final Rietveld refinement plot of GeD_4 at 5 K, showing observed (o), calculated (line) and difference profiles. Vertical bar makers denote calculated Bragg peak positions. The equivalent *d*-spacing range corresponds to 0.83–2.28 Å. Inset: germane molecule showing the atom-labelling scheme.

gas-inlet line based on a design by Langel *et al.* (1986). The gas is deposited at a controlled low rate (20–60 $cm^3\ min^{-1}$ at standard temperature and pressure) in a standard cylindrical vanadium sample tube (diameter 15 mm, height 40 mm) attached to a copper heat sink. A low rate of deposition is essential in order to keep the heat dissipation during condensation to a minimum and thus prevent the powder from annealing or melting. Approximately 2 g of GeD_4 were condensed at 65 K and some 2 g of SnD_4 were condensed at 75 K; these temperatures correspond to $\sim 0.6 \times T_{mp}$ of each compound at which point there is negligible vapour pressure. The samples were then cooled slowly to 5 K for the diffraction measurements.

2.2. Neutron powder diffraction measurements

Time-of-flight neutron powder diffraction data were collected on the high-resolution powder diffractometer (HRPD; Ibberson *et al.*, 1992) at the ISIS pulsed neutron source. For the present experiments at backscattering ($\langle 2\theta \rangle$ = 168°) two time-of-flight ranges were used, 30–130 and 110–210 ms, corresponding to a total *d*-spacing range of ~0.6–4.2 Å. Under these experimental settings the diffraction data have an approximately constant resolution of $\Delta d/d = 8 \times 10^{-4}$. HRPD has additional detector banks at 90 and 30°, which significantly extend the range of *d*-spacings which are accessible; however, these data were not required in the present studies. Diffraction data were recorded on both compounds at the condensation temperature for a brief period and then at 5 K for a period of some 12 h. Both samples were weakly scattering and insufficient beamtime was available in order to carry out measurements as a function of temperature. A standard data reduction procedure was followed: the data were normalized to the incident-beam monitor profile and corrected for the effects of detector efficiency as a function of neutron wavelength using a previously recorded vanadium spectrum.

2.3. Structure solution and refinement

For both samples, the first 25 low-order Bragg reflections ($1.5 < d < 4.0$ Å) at the condensation temperature were located by visual inspection, to an accuracy of 0.001 Å, and the unit cell determined using the auto-indexing program *DICVOL* (Boultif & Louër, 2004) and also using *TOPAS-Academic* (Coehlo, 2008). In each case solutions with a high figure of merit were obtained and these cell parameters were readily refined against the 5 K data indicating no structural phase transitions had occurred on cooling. A primitive orthorhombic cell was determined for germane and a C-centred monoclinic cell in the case of stannane (Table 1). There were a number of unindexed lines corresponding to contaminant scattering from copper and vanadium from the centre stick and the strongest of these peaks were excluded during subsequent analysis. The stannane data also contained additional weak diffraction peaks most likely attributable to decomposition products from the sample.

Density considerations suggest that there are four GeD_4 molecules in the unit cell which implies a non-centrosymmetric orthorhombic space group, assuming the structure comprises one molecule on a general position in the asymmetric unit. The highest-symmetry space group consistent with the systematic absences is $P2_12_12_1$. Using this space group the crystal structure was solved by simulated annealing implemented by *TOPAS-Academic* using an ideal GeD_4 tetrahedral molecular template with a Ge—D bond length of 1.515 Å, as determined by microwave spectroscopy (Ohno *et al.*, 1986). The inherent peak overlap in powder diffraction patterns, even with high-resolution data, often leads to ambiguity in the space-group assignment and hence checks were also made, without success, using other possible space groups, namely $Pmm2_1$, $P2_12_12$, $P222_1$ and $P222$. The final structure[1] was refined without constraints (details are given in Table 1) and the final profile fit is shown in Fig. 1.

[1] Supplementary data for this paper are available from the IUCr electronic archives (Reference: WS5063). Services for accessing these data are described at the back of the journal.

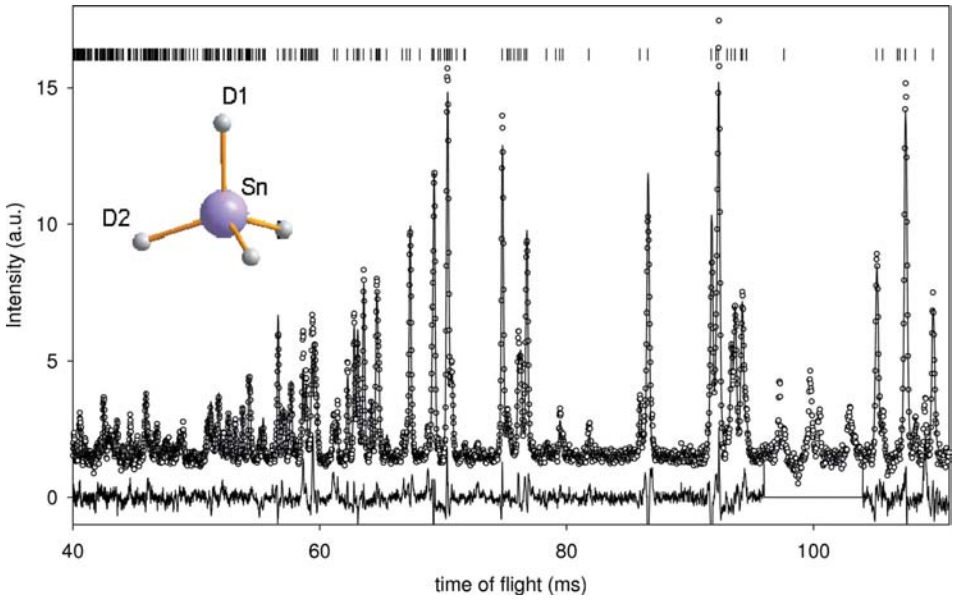

Figure 2
The final Rietveld refinement plot of GeD_4 at 5 K, showing observed (o), calculated (line) and difference profiles. Vertical bar makers denote calculated Bragg peak positions. The equivalent *d*-spacing range corresponds to 0.83–2.24 Å. Inset: stannane molecule showing the atom-labelling scheme.

A similar strategy was adopted in the structure solution of SnD_4. It was deduced that $Z = 4$ and therefore the structure comprises one molecule located either on a general position or located on a twofold rotation axis for the candidate non-centrosymmetric or centrosymmetric space groups, respectively. The structure was solved in the space group $C2/c$ using a molecular template with a Sn—D bond length of 1.694 Å (Ohno *et al.*, 1986). Refinement details are given in Table 1 and the final profile fit is shown in Fig. 2.

Crystal structures were visualized using the program *DIAMOND* (Crystal Impact, 2004) and analyses were carried out using *PLATON* (Spek, 2003).

3. Results and discussion

The low-temperature crystal structure of GeD_4 is represented in Fig. 3. In the structure the molecules pack with no contact distances less than the sum of the van der Waals radii. The shortest contact is D3···D4 at 2.537 (6) Å and links the molecules in zigzag chains running parallel to the crystallographic *b* axis, as shown in the figure. Germane molecules are located on general positions in the structure and exhibit only a small distortion from ideal tetrahedral symmetry with an angular variance of 3.93 deg^2. The average Ge—D bond length is 1.517 Å, r.m.s. deviation 0.015 Å, and in close agreement with the equilibrium distance of 1.516 (5) Å determined by microwave measurements (Ohno *et al.*, 1986). The C_1 site symmetry of the germane molecule in the structure confirms the observations of earlier IR spectroscopy measurements for this phase (Oxton, 1977; Calvani *et al.*, 1990).

The low-temperature crystal structure of SnD_4 is represented in Fig. 4. The average intramolecular Sn—D bond length is 1.707 Å, r.m.s. deviation 0.013 Å, again in close agreement with the equilibrium distance of 1.694 (8) Å determined by microwave measurements (Ohno *et al.*, 1986). The stannane molecules lie on twofold rotation axes and the C_2 site symmetry of the molecule provides for the only negligible angular distortion from tetrahedral symmetry. Short contacts are made between Sn atoms and neighbouring D atoms located over the faces of the molecular tetrahedra comprising the structure. The resulting three-dimensional network has Sn···D1 and Sn···D2 contacts of 3.377 (3) and 3.439 (3) Å, respectively. This facet of the stannane structure also corroborates the results of an IR spectroscopic study (McKean & Chalmers, 1967) in which the spectra of SnH_4 in an GeH_4 matrix, or GeH_4 in an SnH_4 matrix, showed that the normally IR-inactive ν_1 mode of the probe molecule was observed in these matrices. McKean & Chalmers (1967) suggested that an interaction between an *M* atom and one or more H atoms from adjacent MH_4 molecules could account for this increased intensity whilst noting that it

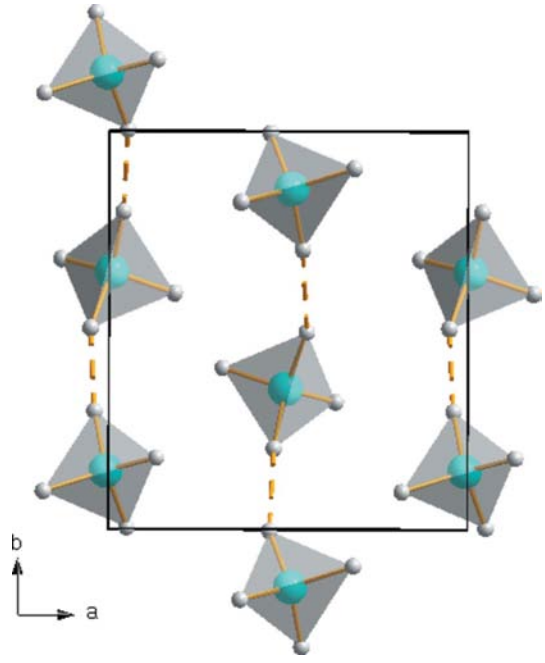

Figure 3
The structure of germane. Dotted lines denote the shortest D···D contacts linking the molecules in chains.

was strange that all four H atoms did not behave similarly, unless there is directional character associated with this close contact.

Voronoi–Dirichlet partitioning (Peresypkina & Blatov, 2000) reveals that the molecular coordination number in both germane and stannane is 14, and the topology is approximately body-centred cubic packing with coordination sequences of 14-52-116 and 14-52-114, respectively. Methane is the simplest tetrahedral molecule for comparison of these packing sequences and, by contrast, the fully ordered low-temperature orthorhombic structure of methane-III (Neumann *et al.*, 2003) exhibits ideal cubic close packing with the coordination sequence 12-42-92, reflecting the more efficient packing of the smaller and more rigid molecules. The structures and phase diagram of silane, SiD_4, were also compared with those of methane by Legrand & Press (1976), who concluded that there was no analogy between silane phases and the three ambient-pressure phases of methane, despite the tetrahedral nature of the molecules in each case. It is also clear from the present measurements that any analogy between the phases of methane with germane and stannane are similarly unlikely to hold true, although detailed crystallographic information regarding the higher-temperature phases is still required. The structures of methane are stabilized primarily through orientationally dependent electrostatic octupole–octupole interactions. However, for silane, germane and stananne, as the molecules become progressively larger it seems probable that van der Waals interactions between the molecular centres become dominant. From consideration of the gas-phase equilibrium structures, similarities are more likely to be observed between silane and germane with Si—H and Ge—H bond lengths of 1.473 and 1.515 Å, respectively (Ohno *et al.*, 1986). Phase III of SiH_4 is stable below 38 K (Wilde & Srinivasan, 1975); however, Legrand & Press (1976) were unable to assign unit cells to their low-temperature neutron powder diffraction patterns of SiD_4 due to limitations in resolution and counting statistics. In light of the present studies, an examination of the SiD_4-III data presented in their paper indicates it is likely to be isostructural with GeD_4-III with lattice constants $a = 7.26$, $b = 8.21$, $c = 4.44$ Å, and a unit-cell volume of 265 Å^3 at 26 K (see supplementary material). Spectroscopic investigations on silane phase III (McKean & Chalmers, 1967; Calvani *et al.*, 1990, 1991) also suggest C_1 molecular site symmetry analogous to the germane structure.

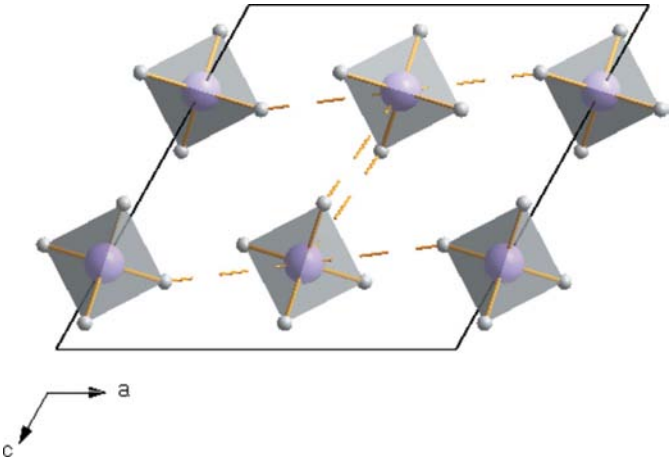

Figure 4
The structure of stannane. Dotted lines denote the direction of intermolecular interactions between Sn atoms and D atoms from neighbouring molecules located over the tetrahedral faces of the molecules.

In summary, the low-temperature phase III structures of perdeuterogermane and -stannane have been determined by high-resolution neutron powder diffraction. Germane has an orthorhombic structure comprising molecules with C_1 site symmetry and this structure is most likely adopted by silane below 38 K. The structure of stannane is monoclinic with molecules located on twofold rotation axes.

This work has been supported by STFC with the provision of neutron beamtime and EPSRC with studentships (IJM and DHB). The authors thank Mr John Dreyer for help with the gas-handling apparatus and Professor Simon Parsons for assistance in attempts to grow single crystals at low temperature.

References

Aldridge, S., Blake, A. J., Downs, A. J., Gould, R. O., Parsons, S. & Pulham, C. R. (1997). *J. Chem. Soc. Dalton Trans.* pp. 1007–1012.
Ashcroft, N. W. (2004). *Phys. Rev. Lett.* **92**, 187002.
Blake, A. J., Ebsworth, E. A. V. & Dyrbusch, M. (1987). *Acta Cryst.* C**43**, 1683–1685.
Boese, R. & Nussbaumer, M. (1994). *Correlations, Transformations, and Interactions in Organic Crystal Chemistry*, edited by D. W. Jones & A. Katrusiak, IUCr Crystallographic Symposia, Vol. 7, pp. 20–37. Oxford University Press.
Boultif, A. & Louër, D. (2004). *J. Appl. Cryst.* **37**, 724–731.
Calvani, P., Ciotti, C., Cunsolo, S. & Lupi, S. (1990). *Solid State Commun.* **75**, 189–192.
Calvani, P., Lupi, S. & Ciotti, C. (1991). *J. Chem. Phys.* **94**, 52–57.
Clusius, K. & Faber, G. (1942). *Z. Phys. Chem. Abt. B*, **51**, 352–370.
Coehlo, A. A. (2008). *Topas-Academic*, http://members.optusnet.-com.au/alancoelho/.
Crystal Impact (2004). *DIAMOND*, Version 3.0. Crystal Impact GbR, Bonn, Germany; http://www.crystalimpact.com/diamond.
Degtyareva, O., Canales, M. M., Bergara, A., Chen, X. J., Song, Y., Struzhkin, V. V., Mao, H. K. & Hemley, R. J. (2007). *Phys. Rev. B*, **76**, 064123.
Downs, A. J., Parsons, S., Pulham, C. R. & Souter, P. F. (1997). *Angew. Chem.* **36**, 890–891.
Feng, J., Grochala, W., Jaron, T., Hoffmann, R., Bergara, A. & Ashcroft, N. W. (2006). *Phys. Rev. Lett.* **96**, 017006.
Hovi, V., Lahteenmaki, U. & Tuulensuu, R. (1969). *Phys. Lett. A*, **29**, 520–521.
Ibberson, R. M., David, W. I. F. & Knight, K. S. (1992). Report RAL-92-031. Rutherford Appleton Laboratory, Oxon, England.
Langel, W., Kollhoff, H. & Knözinger, E. (1986). *J. Phys.* **19**, 86–87.
Legrand, E. & Press, W. (1976). *Solid State Commun.* **18**, 1353–1355.
Li, Z., Yu, W. & Jin, C. Q. (2007). *Solid State Commun.* **143**, 353–357.
Martinez-Canales, M., Bergara, A., Feng, J. & Grochala, W. (2006). *J. Phys. Chem. Solids*, **67**, 2095–2099.
McKean, D. C. & Chalmers, A. A. (1967). *Spectrochim. Acta A*, **23**, 777–798.
Mountfield, K. R. & Weir, R. D. (1978). *J. Chem. Phys.* **69**, 774–784.

Neumann, M. A., Press, W., Noldeke, C., Asmussen, B., Prager, M. & Ibberson, R. M. (2003). *J. Chem. Phys.* **119**, 1586–1589.
Niemela, L. (1973). *Phys. Lett. A*, **43**, 343–344.
Niemela, L., Lahteenm, U. & Hirvonen, M. (1972). *Phys. Lett. A*, **39**, 323–324.
Ohno, K., Matsuura, H., Endo, Y. & Hirota, E. (1986). *J. Mol. Spectrosc.* **118**, 1–17.
Oxton, I. A. (1977). *J. Mol. Struct.* **41**, 195–201.
Peresypkina, E. V. & Blatov, V. A. (2000). *Acta Cryst.* B**56**, 501–511.
Sears, W. M. & Morrison, J. A. (1975). *J. Chem. Phys.* **62**, 2736–2739.
Spek, A. L. (2003). *J. Appl. Cryst.* **36**, 7–13.
The, N. D., Gagnon, J. M., Belzile, R. & Cabana, A. (1974). *Can. J. Chem.* **52**, 327–335.
Tse, J. S., Yao, Y. & Tanaka, K. (2007). *Phys. Rev. Lett.* **98**, 117004.
Wilde, E. & Srinivasan, T. K. K. (1975). *J. Phys. Chem. Solids*, **36**, 119–122.